*8456–8464* *Nucleic Acids Research, 2016, Vol. 44, No. 17* *Published online 2 August 2016*
*doi: 10.1093/nar/gkw696*

# Effect of magnesium ions on the structure of DNA thin films: an infrared spectroscopy study

**Kristina Serec[1,*], Sanja Dolanski Babić[1,*], Rudolf Podgornik[2,3] and Silvia Tomić[4]**

[1]Department of Physics and Biophysics, School of Medicine, University of Zagreb, Zagreb, 10000, Croatia, [2]Department of Theoretical Physics, J. Stefan Institute, Ljubljana, 1000, Slovenia, [3]Department of Physics, Faculty of Mathematics and Physics, University of Ljubljana, Ljubljana, 1000, Slovenia and [4]Institute of Physics, Zagreb, 10000, Croatia

Received April 12, 2016; Revised July 12, 2016; Accepted July 27, 2016



## ABSTRACT

**Utilizing Fourier transform infrared spectroscopy we have investigated the vibrational spectrum of thin dsDNA films in order to track the structural changes upon addition of magnesium ions. In the range of low magnesium concentration ([magnesium]/[phosphate] = [Mg]/[P] < 0.5), both the red shift and the intensity of asymmetric $PO_2$ stretching band decrease, indicating an increase of magnesium-phosphate binding in the backbone region. Vibration characteristics of the A conformation of the dsDNA vanish, whereas those characterizing the B conformation become fully stabilized. In the crossover range with comparable Mg and intrinsic Na DNA ions ([Mg]/[P] ≈ 1) B conformation remains stable; vibrational spectra show moderate intensity changes and a prominent blue shift, indicating a reinforcement of the bonds and binding in both the phosphate and the base regions. The obtained results reflect the modified screening and local charge neutralization of the dsDNA backbone charge, thus consistently demonstrating that the added Mg ions interact with DNA via long-range electrostatic forces. At high Mg contents ([Mg]/[P] > 10), the vibrational spectra broaden and show a striking intensity rise, while the base stacking remains unaffected. We argue that at these extreme conditions, where a charge compensation by vicinal counterions reaches 92–94%, DNA may undergo a structural transition into a more compact form.**

## INTRODUCTION

Negatively charged (bio)polymers, such as double stranded deoxyribonucleic acid (dsDNA), are among the fundamental components of the biological milieu and their charge-derived properties are in direct relation to their structural properties and biological functions (1). Major experimental and theoretical studies consistently show that inter-polyion forces depend on polymer length and concentration, added salt concentration and the nature of the mobile ions, intrinsic or provided by the added salt. It is important to note that the cations in particular play a critical role in determining the details of the polyion-polyion interactions: in the presence of weakly electrostatically coupled monovalent and divalent cations, the dominant interaction is repulsive, modified by partial neutralization of the polyion negative charge and Debye screening. Higher valency cations act altogether differently, and can engender attractive interactions between nominally equally charged polyions due to the strong electrostatic coupling effects (2). In the weak coupling scenario, one distinguishes two screening limits yielding two basically different results: in the low screening limit, the polymers remain stretched and statistically assume an extended, rod-like configuration, whereas in the high screening limit they persist in an ideal polymer configuration, best described as either a self-avoiding walk or a ideally random walk (3–6). These results, strictly valid for the bulk remain however valid also for adsorbed DNA (7) and by analogy can be presumed to hold also for surface deposited DNA solutions. In the strong coupling scenario, the correlation effect of the polyvalent counterions strongly reduces the rigidity of charged polymers which then further collapse into highly compact states (8,9), with distinct morphology as is the case of dsDNA toroids (10).

dsDNA presents a prominent example of a complex solution behavior due to its stiffness and in particular the strong electrostatic interactions: in aqueous solutions *in vitro*, it assumes the conformation of an extended statistical coil, whereas *in vivo* long genomic DNA is folded into dense and compact states to fit within the micron-sized nucleus of eukaryotic cells or even smaller nano-scale viral capsids (11,12). To a large degree the behavior seen *in vivo* can be closely reproduced *in vitro* either by tuning the DNA concentration via an applied osmotic stress, by varying the

*To whom correspondence should be addressed. Tel: +385 14566761; Fax: +385 14590276; Email: kristinaserec@gmail.com
Correspondence may also be addressed to Sanja Dolanski Babić. Email: sanja.dolanski.babic@gmail.com

amount of added salt, and/or by increasing the valency of the cations. It is well known that the conformational properties of cellular components play a key role in determining their functional behavior and over the years much effort has been invested to improve a description and understanding of DNA structural features in diverse environments. Despite numerous experimental and theoretical studies by X-ray crystallography, nuclear magnetic resonance, infrared spectroscopy, intensive all atom or coarse grained molecular simulations and quantum chemical calculations, the base pairing and stacking interactions, responsible for the dsDNA structure, are still not understood in all the relevant details (11,13–19).

The role of cation-mediated interactions is another open issue. Investigations over many years by various techniques including circular dichroism spectroscopy, UV-visible spectrophotometry, sedimentation equilibrium measurements, Raman and infrared spectroscopy (20–24) identified main interaction sites at the phosphate groups, and at the electron-donor groups of the bases such as carbonyl groups and nitrogen atoms, and showed that the interactions between the cations and the DNA helix strongly depend on the nature of the cation, its concentration and its hydration state. Distinct binding mechanisms were suggested, involving not only electrostatic but also direct site-specific interactions pending on the hydration and charge of the cation (23). Some divalent cations, such as alkaline-earth $Mg^{2+}$ and $Ca^{2+}$, were suggested to interact purely electrostatically with negatively charged phosphates, rather than with specific nitrogen base sites, and consequently locally neutralize the negative dsDNA backbone charge and in this way stabilize the double-helix secondary structure (25). However, conflicting interpretations were suggested involving either non-specific (23,26), or site-specific (21) long-range electrostatic interactions, or site-specific chemical binding envisioned even as a direct covalent binding (27). Importantly, recent theoretical studies give strong evidence suggesting minor if any site specific binding (28,29). On the other hand, divalent cations like transition-metal $Mn^{2+}$ and $Zn^{2+}$ were shown to bind preferably to base sites in a direct covalent-like manner, inducing conformational changes of the native structure related to their binding. However, these apparent differences between different cations may also be due to the fact that most of the studies were conducted at different conditions, including several orders of magnitude different DNA concentrations, as well as differing cation concentration ranges.

In order to address how the behavior of DNA evolves upon progressive addition of $Mg^{2+}$ cations, we have performed an extensive investigation of infrared vibrational properties of dsDNA in a broad range of added magnesium chloride salt concentration with cation/phosphate ratio between 0.0067 and 30. To be able to make relevant comparisons with previous reports, we have studied native surface deposited DNA using a Fourier transform infrared spectroscopy, widely recognized as a non-destructive and powerful technique to probe vibrational features of DNA that are tightly connected to its structural properties. Our results demonstrate that going from the low to the high magnesium content, cation–DNA interaction changes in strength due to enhanced screening, present in the both the backbone as well as the base regions. Whereas lower $Mg^{2+}$ salt concentrations stabilize the double-helix B conformation of dsDNA, extremely high non-physiological contents, larger than 150 mM, induce fundamental modifications of the secondary structure. Possible interpretations of the observed behavior are discussed and the arguments are provided that an electrostatic interaction/binding is the most relevant mechanism for the observed interaction of magnesium ions with DNA. At extremely large $Mg^{2+}$ contents, a possibility of Mg-induced DNA transition into a compact form is discussed.

## MATERIALS AND METHODS

Salmon testes lyophilized Na-DNA threads were purchased from Sigma-Aldrich. Previous gel electrophoresis measurements showed that the majority fragments were in the 2–20 kbp range, implying the contour length between 0.7 and 7 μm; so that the estimated average DNA fragments were 4 μm long (30). Low protein content was declared and verified by our UV spectrophotometry measurements as $A_{260}/A_{280} = 1.8–2.0$. Ultrapure MilliQ water (labeled as pure water throughout the paper) with declared conductivity 0.056 μS/cm was used in all experiments.

Dry Na–DNA threads were dissolved in pure water for 48 h at 4 °C with occasional stirring to ensure the formation of homogeneous solution. The solutions of $MgCl_2$ were prepared in pure water and added dropwise to the DNA solutions to attain desired cation/phosphate $r = [Mg]/[P]$ molar concentration ratio: 0.0067, 0.01, 0.02, 0.07, 0.15, 0.3, 0.5, 0.67, 1, 1.5, 2, 3.3, 5, 10, 20 and 30, at a final DNA concentration of 7.5 mM. In addition, pure water Na–DNA solution with molar concentration of 7.5 mM was prepared as a reference. For comparison, we have also prepared DNA solution in 10 mM NaCl. Reference solutions pH was 7, while for all other solutions prepared with different ratios $r = [Mg]/[P]$, pH was $6.0 \pm 0.5$. In order to avoid complications arising in the presence of ions of different size and charge (31), and to conduct FTIR measurements in well defined conditions with only intrinsic sodium DNA and added magnesium cations present, no buffers were added.

UV spectrophotometry measurements of the DNA absorbance intensity at 260 nm were done in order to verify the nominal DNA concentration. The concentration was determined assuming double-stranded conformation, using the extinction coefficient at 260 nm equal to 20 L/gcm. Approximately 80% of the wei ght is associated with DNA and the remaining 20% is due to water and intrinsic counterions (32). Throughout the paper, we will refer to these measured concentrations as the 'DNA concentrations'. We have also used UV spectrophotometry in order to verify the stability of the double-stranded conformation (dsDNA) of samples studied by FTIR. The results showed, consistently with previous reports (32–34), the absence of denaturating changes for all samples studied by FTIR which were prepared from solutions whose DNA concentration (i.e. concentration of intrinsic DNA counterions) was 0.15 mM or larger.

In order to obtain thin films, 30 μL of the respective DNA stock solutions with final DNA molar concentrations of 7.5 mM were deposited on optical grade silicon transmission windows and dried in a desiccator for 10 min using rotary

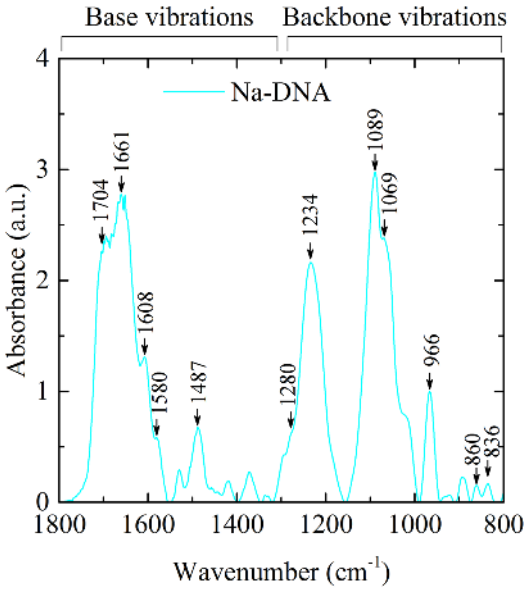


**Figure 1.** FTIR spectra of Na–DNA thin film in the region 800–1800 $cm^{-1}$ measured at about 85% r.h. Labels identify bands assigned to the specific base and backbone (sugar and phosphate) vibrations (see main text).

vacuum pump. Reference film was obtained from pure water Na–DNA solution with molar concentration of 7.5 mM. Throughout the paper, this reference spectrum will be referred to as Na–DNA. For comparison, we also prepared thin films of DNA in 10 mM NaCl in the same manner. Estimated relative humidity of prepared thin films, Na–DNA, as well as those with added salt, was close to 85% r.h. (35).

Fourier transform infrared spectroscopy (FTIR) spectra of thin films were recorded on PerkinElmer Spectrum GX spectrometer equipped with nitrogen cooled MCT detector and KBr beam splitter. The current experimental setup is adapted for DNA thin film experiments in order to avoid problems with water subtraction, especially in the base region. The spectra were taken within 30 minutes after obtaining a thin film, once we verified that essentially the same result was obtained after 120 and 240 min. Spectra were measured at 25 °C and recorded in transmission mode with 4 $cm^{-1}$ resolution and 64 co-added scans and later processed in Kinetics add on for Matlab 2010. Raw data were baseline-corrected and normalized using the band at 966 $cm^{-1}$ (deoxyribose C-C stretching mode) as internal reference because it showed negligible spectral changes in position or intensity upon cation complexation (26,36,37). The spectra were measured as a function of [Mg]/[P] ratio with reproducibility of ±0.1%.

## RESULTS

### Na-DNA

The reference thin film vibrational spectrum of Na-DNA, measured in the spectral range between 800 and 1800 $cm^{-1}$, is presented in Figure 1. Besides vibrations due to DNA base-pair interaction in the range 1300–1800 $cm^{-1}$, we observe also characteristic features of the sugar and phosphate DNA backbone vibrations in the range 800–1300 $cm^{-1}$ (17). Our results are fully consistent with previous FTIR measurements on films (25,38–40), as well as on aqueous solutions (26,36,41).

In particular, the main absorption bands associated with DNA bases are the carbonyl C=O and C=N in-plane stretching modes. The former vibrations, commonly considered to originate in guanine bases (C6=O6) and thymine bases (C2=O2), are centred at 1704 $cm^{-1}$, while vibrations in thymine bases (C4=O4) are centred at 1661 $cm^{-1}$. The latter vibrations, considered to originate in adenine bases (C8=N7), are centred at 1608 $cm^{-1}$, and those originating in the cytosine bases (C4=N3) and guanine bases (C8=N7) are centred at 1487 $cm^{-1}$ (13,15,42,43). The most prominent phosphate and sugar stretching vibrations are asymmetric and symmetric $PO_2$ stretching modes at 1234 and at 1089 $cm^{-1}$, respectively, sugar-phosphate stretching bands at 1069 and at 893 $cm^{-1}$, and deoxyribose stretching mode at 966 $cm^{-1}$. A deoxyribose-thymine band can be also recognized as a high-frequency shoulder at 1280 $cm^{-1}$. The sugar-phosphate bands, considered as the most important markers pertaining to B and A conformations of dsDNA, are visible at 836 and 860 $cm^{-1}$, respectively (14). A comparison of the integrated absorptions of these bands $A_{836}/(A_{836} + A_{860})$ (44,45) gives the fraction of B form of about 54%. A possible signature of the A form is identified at 1069 $cm^{-1}$ thus hindering a 1055 $cm^{-1}$ band, a fingerprint of the B form DNA. Therefore, our spectra shown in Figure 1 indicate a modified B form dsDNA structure, leaning toward the A form dsDNA (26). Two additional spectral features would corroborate this interpretation: the guanine band found at 1704 $cm^{-1}$, instead at 1717 $cm^{-1}$, and the asymmetric $PO_2$ stretching mode at 1234 $cm^{-1}$, usually found in the range at 1220–1225 $cm^{-1}$. Our findings are in accord with the previous FTIR studies which showed these changes in Na-DNA even for relative humidity levels as high as 90% r.h. (35,38,40). Furthermore, as we will show in the next section, spectral signatures of the A form diminish with increasing magnesium content $r$ = [Mg]/[P], and eventually completely disappear for $r \approx 0.5$. The position of asymmetric $PO_2$ concurrently shifts to lower values down to 1229 $cm^{-1}$; a slightly higher frequency is due to an initially lower salinity of Na–DNA films in our work (46).

### DNA in $MgCl_2$

In what follows, we present results of the infrared response performed on thin films of dsDNA containing magnesium ions. The spectra were taken as a function of $r$ = [Mg]/[P] ratio in the range $0.0067 \leq r \leq 30$. We can identify three regions with different levels of Mg content characterized by distinct spectral changes: the region of low Mg content, $0.0067 \leq r < 0.5$, medium Mg content $0.5 \leq r < 5$ ($r \approx 1$), and high Mg content $r \geq 5$–10. The representative spectra for the regions of low, medium and high Mg content are displayed in Figures 2 and 3. These spectra show that in the presence of magnesium ions, the DNA infrared signatures are perturbed extensively, in particular for the case of high Mg content.

First, we address the case of low and medium Mg content (Figure 2). In the $0.0067 \leq r < 0.5$ the most noticeable changes are found in the backbone region and con-

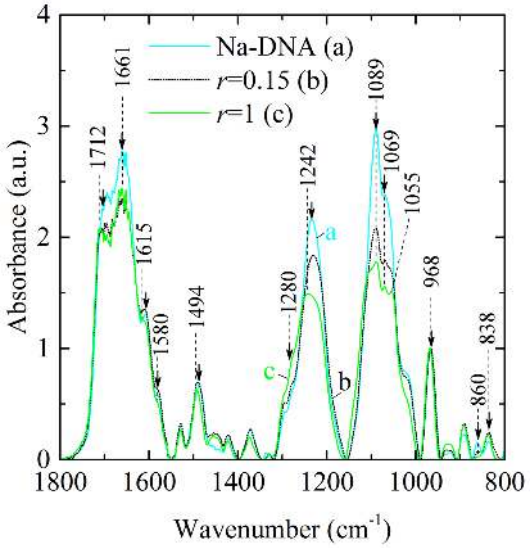


**Figure 2.** FTIR spectra of DNA thin films in the region 800–1800 $cm^{-1}$ measured at about 85% r.h. for representative Mg content $r = [Mg]/[P]$: 0.15 (b—black, dotted) and 1 (c—green). Labels (dashed lines and numbers) identify bands undergoing prominent changes for $r = 1$. Reference spectrum of Na–DNA is shown for comparison (a—blue): vibrational bands, assigned to the base and backbone vibrations, are marked by arrows.

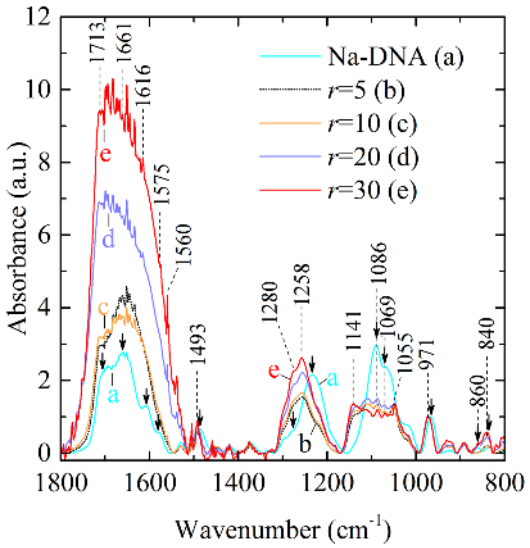


**Figure 3.** FTIR spectra of DNA thin films in the region 800–1800 $cm^{-1}$ measured at about 85% r.h. for representative Mg content $r = [Mg]/[P]$: 5 (b—black, dotted), 10 (c—orange), 20 (d—purple) and 30 (e—red). Labels (dashed lines and numbers) identify bands undergoing prominent changes for r = 30. Reference spectrum of Na–DNA is shown for comparison (a—blue): vibrational bands, assigned to the base and backbone vibrations, are marked by arrows.

cern a major drop in intensity of asymmetric $PO_2$ stretching band at 1234 $cm^{-1}$ (Figure 4, upper panel), of the symmetric $PO_2$ stretching band at 1089 $cm^{-1}$, as well as of the sugar-phosphate stretching band at 1069 $cm^{-1}$, considered as a fingerprint of the A form (see Figure 2). The observed intensity changes happen concomitantly with a red shift of asymmetric $PO_2$ stretching band from 1234 to 1229 $cm^{-1}$ (Figure

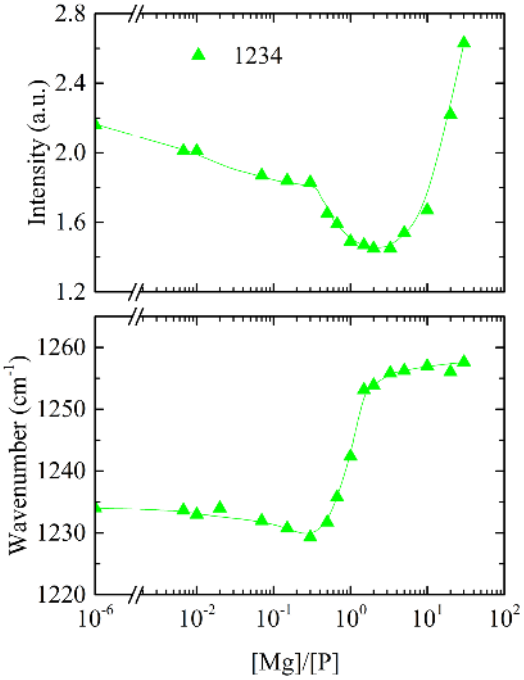


**Figure 4.** Intensity (upper panel) and frequency position (lower panel) of the asymmetric $PO_2$ stretching band, centred at 1234 $cm^{-1}$ for Na-DNA, as a function of Mg content $r = [Mg]/[P]$. Data point for $r = 10^{-6}$ corresponds to Na–DNA. Full lines are guides for the eye.

4, lower panel), which indicates an increasing magnesium-phosphate binding upon addition of Mg ions. Another important effect of increasing Mg content in this region occurs at sugar-phosphate bands at 836 $cm^{-1}$ (B marker) and at 860 $cm^{-1}$ (A marker). Remarkably, the intensities of A and B markers concurrently change in opposite directions (Figure 5); the B form becomes fully stabilized for $r \approx 0.5$ (calculated B form fraction from the integrated intensities is ~95%), as testified by an almost complete disappearance of the A form marker at 860 $cm^{-1}$, and by a significant decrease of the band at 1069 $cm^{-1}$, accompanied by an appearance of a shoulder at 1055 $cm^{-1}$ associated with the sugar vibration characteristic of B form (Figure 2). In the base region, spectral changes include a small decrease in intensity of bands due to C=O in-plane stretching modes at 1704 and 1661 $cm^{-1}$, while the effect is barely detectable for the C=N bands at 1608 and 1487 $cm^{-1}$. Importantly, no major shift in the frequency position is found, except for the C=N vibration at 1487 $cm^{-1}$. These changes indicate the appearance of a weak association between Mg ions and nitrogen bases, that nevertheless remains of minor importance as compared to the overwhelming Mg localization in the vicinity of the backbone phosphates, due to unspecific electrostatic interactions (27). Overall changes at low contents ($0.0067 \leq r < 0.5$) thus indicate that Mg is preferably localized in the vicinity of the phosphate groups, locally screening their charge and in this way inducing increased base stacking interactions which furthermore stabilize the B form of dsDNA. Our results are in pleasing agreement also with previously obtained FTIR (25) and Raman (27) experiments and extend their validity throughout the low range

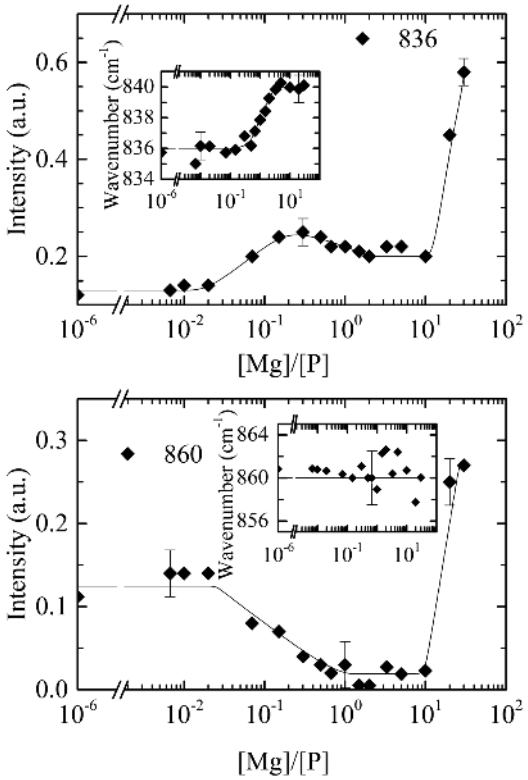


**Figure 5.** Intensity and the frequency position (insets) of the B marker at 836 $cm^{-1}$ for Na–DNA and of the A marker at 860 $cm^{-1}$ as a function of Mg content $r = [Mg]/[P]$ are shown in upper and lower panel, respectively. Data point for $r = 10^{-6}$ corresponds to Na-DNA. Full lines are guides for the eye.

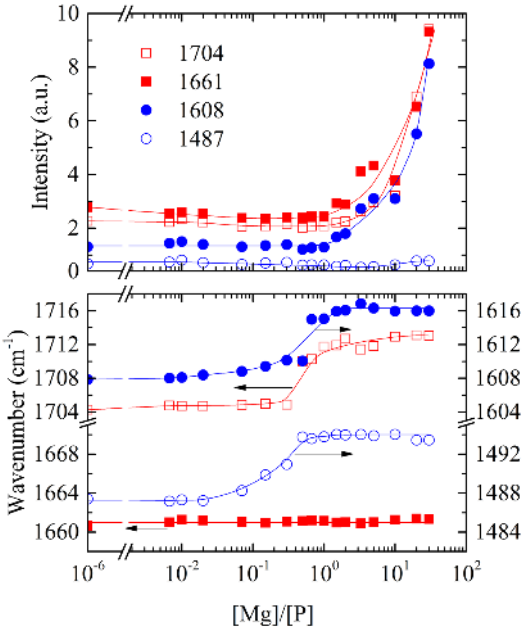


**Figure 6.** Intensity (upper panel) and frequency position (lower panel) of the most important vibrations bands in the base region for Na–DNA as a function of Mg content $r = [Mg]/[P]$. The C=O band at 1704 $cm^{-1}$ (open red squares) and at 1661 $cm^{-1}$ (full red squares); the C=N band at 1608 $cm^{-1}$ (full blue circles) and at 1487 $cm^{-1}$ (open blue circles). For details of assignments, see main text. Data point for $r = 10^{-6}$ corresponds to Na–DNA. Full lines are guides for the eye.

of the Mg content. Finally, concerning a direct Mg-N7 guanine specific, 'chemical' binding, observed by FTIR measurements in solution (26), and suggested to occur on the basis of spectral changes observed at very low Mg contents ($r = 0.0125$), we note that a direct cation-nitrogen base specific chemical binding is expected for transition metal ions with partially filled d-orbitals, but it would be difficult to rationalize for divalent Mg ions. In any case, we consider that the perturbation on the N7 guanine site in the presence of alkaline-earth metal ions, if any, should be weaker and only indirect in nature (27,28).

In the medium range, $0.5 \leq r < 5$, the B conformation continues to be stable. However, new important spectral changes occur in the base region, indicating the incipient magnesium binding in the base region. Namely, the modes associated with the C=N vibrations (centred at 1608 $cm^{-1}$ in Na–DNA) and with the C=O vibrations (centred at 1704 $cm^{-1}$ in Na–DNA) show minor intensity increase accompanied by a strong blue shift from 1608 and 1704 $cm^{-1}$ to 1616 and 1713 $cm^{-1}$, respectively (Figure 6). On the other hand, the C=O band centred at 1661 $cm^{-1}$ in Na-DNA gains intensity but shows also no displacement in frequency, while C=N band centred at 1487 $cm^{-1}$ in Na–DNA shows a major frequency shift from 1487 to 1494 $cm^{-1}$, but with no intensity change. It is noteworthy that these effects occur concomitantly with the blue shift of bands in the backbone region. The B marker shows a small shift to higher frequencies and saturates at 840 $cm^{-1}$ for $r \approx 5$ (Figure 5). The asymmetric $PO_2$ stretching mode at 1234 $cm^{-1}$ also shows a shift to higher frequencies, which is accompanied by widening of the band and further, more pronounced, intensity decrease (Figure 4). It is noteworthy that the observed shift to higher frequency is commonly attributed to a decreasing hydrogen bonding of water and taken as a sign of lower hydration level (35), the effect which is excluded here since the hydration level of all our films is always the same. Rather, as we will discuss in the next section, this shift reflects the interaction between Mg ions and DNA upon further addition of Mg ions. The shape of this band also suggests 3 major contributions centred at 1280, 1242 $cm^{-1}$ and at 1226 $cm^{-1}$ (not indicated in Figure 2). Another observed change concerns the deoxyribose-thymine band visible as a shoulder at 1280 $cm^{-1}$, which shows a large intensity increase for $r = 1$, but no frequency shift (Figure 2). As we will argue later, the observed frequency shifts indicate that a stronger magnesium–DNA interaction develops as compared to the one at low $Mg^{2+}$ contents.

Further addition of $Mg^{2+}$ ions ($r \geq 5$–10) then leads to abrupt changes: the C=O and C=N bands in the base region 1550–1800 $cm^{-1}$, as well as the asymmetric $PO_2$ stretching band in the backbone region present striking jumps in intensity and a significant broadening (Figures 3 and 4 upper panel, Figure 6). We also note the appearance of a band at 1560 $cm^{-1}$ and a prominent intensity rise of the deoxyribose-thymine band at 1280 $cm^{-1}$. On the other hand, in the region of the symmetric $PO_2$ stretching originally centred at 1089 $cm^{-1}$, spectral changes which started

to develop for the low and medium $Mg^{2+}$ content, become only more pronounced with further addition of magnesium ions. Likewise, the deoxyribose stretching mode originally centred at 966 $cm^{-1}$ continuously shifts to 971 $cm^{-1}$ with increasing $Mg^{2+}$ content, therefore indicating only modest structural changes in the region of the sugar-phosphate backbone. Finally, important spectral changes concerning the B and A markers of the DNA conformation should be noted (Figure 5) as for highest Mg contents ($r = 20$ and 30), a prominent intensity jump occurs for both, the B as well as for the A marker. The overall spectral changes in the presence of these high Mg contents thus indicate that magnesium interaction with both, the DNA backbone and the base regions is at the origin of significant changes of the DNA conformation at these non-physiological salinity conditions and, as we will argue later, may be responsible for Mg-induced transition into a more compact form.

## DISCUSSION

We first summarize the main results of infrared measurements and discuss the related structural changes which indicate the nature of interaction between Mg ions and ds-DNA. In the range of low Mg content ([Mg]/[P] < 0.5) our data are in a good agreement with previously obtained results (23,25,26). There are a number of spectral changes which happen simultaneously. The intensity decrease of the asymmetric and the symmetric $PO_2$ stretching bands, accompanied by a red shift, are due to pronounced Mg interaction with the backbone phosphates; the magnitude of these changes is relatively small, pointing to a non-specific electrostatic nature of this interaction, rather than a direct, site-specific binding. In the base region, C=O bands show a small intensity drop, while C=N bands show only a minor blue shift. Vibrations at 860 and 1069 $cm^{-1}$ characteristic of the A conformation of the dsDNA vanish, whereas those characteristic of the B conformation, such as the sugar-phosphate vibration at 836 and 1055 $cm^{-1}$, become fully stabilized. These findings consistently indicate that the binding of magnesium ions in this concentration regime occurs mostly in the region of phosphate groups without any significant perturbation of the DNA bases. Importantly, such predominantly electrostatic interaction/binding gives rise to a decreased effective charge density, as evidenced by the observed shift to lower frequencies of the asymmetric $PO_2$ stretching mode, and thus results in a stronger base-stacking interaction and double-helix stability. This is confirmed also by the observed decrease of intensities of the C=O vibrations in the base region. The implied decrease of the effective charge density through $Mg^{2+}$ concentration-dependent charge compensation is consistent also with the Manning counterion condensation theory in an environment containing two species of cations (47) (see Figure 7 and the related discussion at the end of this section). Namely, while for the one-cation case the Manning theory of the counterion condensation predicts that about 76% and 88% of DNA charge is neutralized by monovalent and divalent cations, respectively (4,47), the outcome of the competition between two different cations is determined not only by the valences, but by their concentrations as well.

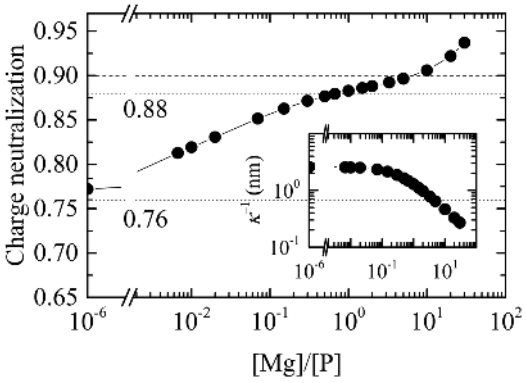


**Figure 7.** Calculated degree of charge neutralization of DNA, i.e. charge compensation by condensed counterions ($\Theta_{Na} + 2\Theta_{Mg}$) and Debye screening length $\kappa^{-1}$ (inset) as a function of Mg content $r = [Mg]/[P]$. Data point for $r = 10^{-6}$ corresponds to Na–DNA. $\Theta_{Na}$ and $\Theta_{Mg}$ stand for the fraction of bound $Na^+$ and $Mg^{2+}$ counterions, respectively. Dotted lines designate expected compensated phosphate charge when only one species of cations is present: $\Theta_{Na} \approx 0.76$ and $\Theta_{Mg} \approx 0.88$. Dashed line designates ($\Theta_{Na} + 2\Theta_{Mg}$) $\approx 0.90$ when the DNA collapse may occur.

On further addition of Mg ions in the medium range $0.5 \leq r < 5$, the B conformation continues to be stable. The intensity of asymmetric $PO_2$ stretching band now decreases at a much faster pace, in the whole interval all the way to $r \approx 5$. Concomitantly, the previously observed trend in the frequency shift is reversed, indicating a stronger Mg-phosphate binding that gradually sets in. The observed spectral changes reveal a higher force constant indicating a steeper potential, reinforcing the vibration of the bonds upon the addition of Mg ions. Prominent blue shifts appear also in the base region and are accompanied with an intensity increase of the C=O band centred at 1704 $cm^{-1}$ in Na–DNA and the C=N band at 1608 $cm^{-1}$. These changes indicate that the range of the magnesium-DNA interaction increases at these higher $Mg^{2+}$ contents. On the other hand, the C=O vibrations centred at 1661 $cm^{-1}$ and C=N vibrations at 1487 $cm^{-1}$ seem to be ruled out from the binding due to missing frequency and intensity changes, respectively. The task then, is to distinguish between the C=O and C=N bonds in the DNA bases, whose excitations induce frequency and intensity changes as a function of $Mg^{2+}$ content, and those which remain silent under infrared irradiation. Based on the previous FTIR studies (see section 'Na–DNA'), we assign the C=N vibrational modes occurring at 1608 $cm^{-1}$ to either C8=N7 bonds in adenine bases or to C6=C5 bonds in thymine bases, while those occurring at 1487 $cm^{-1}$ are assigned to the C4=N3 and the C8=N7 bonds in cytosine and guanine bases, respectively. Remarkably, only the former mode, with contributions situated in the proximity of the sugar-phosphate backbone, is affected by addition of $Mg^{2+}$. On the other hand, the latter mode, resulting from the vibrations in the proximity of the backbone, as well as from vibrations in the interior of cytosine-guanine base pair, is at most blue-shifted, but does not show any intensity change. Likewise, the vibrational mode at 1661 $cm^{-1}$ commonly assigned for the most part to the interior C4=O4 stretches in the thymine bases, shows only an in-

tensity rise, but does not show any frequency shift. Finally, the vibrational mode at 1704 $cm^{-1}$, which is blue-shifted and shows an intensity rise, may be assigned to C2=O2 stretches close to thymine N1 site, where the base is linked to the sugar-phosphate backbone. All these spectral changes demonstrate that $Mg^{2+}$ binding occurs at the level of the DNA backbone and that the $Mg^{2+}$ ions do not penetrate into the interior of the base-pairs. Therefore, any significant influence on the intra-base pairing can be safely excluded.

The overall spectral changes, observed at low and medium Mg contents, reveal that the interaction of magnesium ions with DNA is determined by electrostatic forces, renormalized by the ion atmosphere (48), with their inherent and long-range character. Namely, on increase of the $Mg^{2+}$ ions with $r > 0.5$, when the $Mg^{2+}$ ions prevail over the intrinsic $Na^{1+}$ counterions, the Debye screening length starts to decrease strongly (Figure 7). An additional piece of evidence, which suggests that the localized site-specific $Mg^{2+}$–DNA binding may be safely excluded, is the fact that the vicinal $Mg^{2+}$ ions retain their hydration state and mobility over a wide concentration range (29,48,49).

Finally, in the high Mg content region with $r \geq 5$–10, the vibrational spectra are strongly perturbed: a striking intensity rise and significant broadening is found for the asymmetric $PO_2$ stretching vibrations, as well as for the C=O guanine and thymine, and C=N adenine modes. The intensity changes of B and A markers at 836 and 860 $cm^{-1}$ for highest Mg content indicate that the secondary structure of DNA is strongly modified, suggesting a transition to some intermediate conformation which differs from the common B form geometry. Importantly, only minor additional blue frequency shifts, as compared to the ones found for $0.5 < r < 5$, are detected in this regime, and are primarily observed for the asymmetric $PO_2$ stretching and C2=O2 thymine stretching, amounting at most to 1 $cm^{-1}$. This finding suggests that an almost complete DNA charge compensation as a result of vicinal counterions occurs for $r \approx 5$. Similar drastic increase of the intensities of vibrations in the base and phosphate regions for divalent and trivalent cations such as $Cu^{2+}$, $Pb^{2+}$, $La^{3+}$ have been interpreted by some authors as a signature of the DNA denaturation (50,51). In these cases, the intensity changes were accompanied by red shifts of the base vibrations and blue shifts of the sugar-phosphate backbone band at 1055 $cm^{-1}$, indicating the creation of new binding sites at these cation concentrations. However, these effects were not found in our work. Therefore, although a considerable increase of intensity might point to a double-helix destabilization and base pair openings, our data rule out a major unwinding of the dsDNA as a relevant scenario at high Mg contents. The additional support for this claim comes from the UV measurements, which show a small but clear decrease of the absorption upon addition of Mg ions, indicating stabilization of the dsDNA structure at these extremely high Mg contents (52). We can therefore only reiterate our previous conclusion that for all studied $Mg^{2+}$ contents, any kind of direct, site-specific coordination, known to destabilize intra base-pair hydrogen bonds and base stacking, can be definitively ruled out.

In what follows, we discuss the possibility of a Mg-induced dsDNA transition into a compact form, which sets in once the magnesium/phosphate ratio becomes larger than 10 ($r > 10$). The phase transition interpretation is suggested by the observed highly discrete changes in the intensity of vibration modes and their significant broadening, implying the presence of non-equivalent components. It has been already proposed by various authors before, that divalent cations such as $Mg^{2+}$ at high concentrations of several hundred mM and/or confined in reduced spatial dimensions, could be effective in changing the DNA structure and even induce DNA compactification with different morphologies related to the detailed cation binding position to dsDNA (22,53–55). At extremely high $Mg^{2+}$ concentrations, larger than 150 mM ($r > 10$), a crossover from repulsive to attractive electrostatic interactions between DNA segments may happen, driven by the strong coupling correlation effect (56), even if the $Mg^{2+}$ ions do not directly lead to DNA condensation in the bulk (57). Indeed, structural studies using electron microscopy indicate that $Mg^{2+}$ ions facilitate the close approach of DNA segments, even if they do not explicitly condense it (58). One should however note, that divalent counterions are at the boundary of the strong coupling electrostatics and do not as a rule exhibit the same features as the more highly charged DNA condensing counterions (59). Apart from the strong coupling electrostatics, one should note also the role of hydration forces, associated with the perturbed vicinal water structure, that have been hypothesized to turn from repulsive to attractive, depending on the compensatory nature of the hydration shell of dsDNA and $Mg^{2+}$ ions (22,57). Even a combination of the two effects, water structuring coupled to electrostatic interactions, could just as well lead to water-mediated attractive electrostatic interactions that would show pronounced cation specificity (60).

Finally, we have applied the approximate two-variable Manning approach for a mixture of two types of cations to our DNA system (47,61–63) noting that it corresponds almost quantitatively to a separation of 2 nm away from the surface of DNA if compared to the 'exact' MD simulation predictions (see Figure 3D in (29)). Note that as the concentration of Mg ions increases, so does the charge neutralization by condensed counterions. Recent experiments (31) make it clear that in the case of two different cations in the ionic atmosphere, the higher charge of divalent cations relative to that of monovalent ones, is expected to favor cation association over anion exclusion in DNA neutralization. Thus, we interpret the rising charge neutralization with added Mg in terms of an increase in the number of bound $Mg^{2+}$ ions, and a decrease in the number of bound $Na^{+}$ ions in the ion atmosphere (28). It is gratifying to find that for approximately equal concentrations of $Na^{+}$ and $Mg^{2+}$ ions ($r \approx 1$) the DNA charge is neutralized at the level of 0.88, implying that nearly all of the accumulated bound counterions are divalent $Mg^{2+}$ ions (48). Last but not least, previous calculations based on the Manning approach for a mixture of two cations of different valencies, and invoked in the context of light scattering, UV and FTIR data, have indicated that the DNA collapse can occur when about 90% of DNA charge is neutralized by the vicinal (condensed) counterions (62,63). Remarkably, in our experiments, the 90% local charge compensation has been achieved for added $Mg^{2+}$ concentration of ~150 mM ($r = 10$) (Figure 7), right at the

threshold, above which intriguing spectral changes, indicating an alternation in the DNA structure, make their appearance.

## CONCLUSIONS

We have investigated vibrational spectra of thin DNA films at 85% r.h. using infrared vibrational spectroscopy (800–1800 $cm^{-1}$) in order to investigate structural changes upon addition of magnesium ions in the wide range of $0.0067 \leq r = [Mg]/[P] \leq 30$. Three vibrational bands were identified to undergo the most prominent spectral changes in this range of $r$, revealing the Mg-DNA interactions: the asymmetric $PO_2$ stretching mode (1234), the carbonyl C=O (1704) and the C=N (1608) in-plane stretching mode. In the range of low Mg content ($[Mg]/[P] < 0.5$), vibrational spectra remain almost unchanged in the nitrogen base region, except for a minor intensity drop and a blue shift of the C=N stretching bands. In the phosphate backbone region, the red shift and the intensity decrease of the asymmetric $PO_2$ stretching band can be attributed to a progressive Mg localization in the vicinity of the oppositely charged phosphates that increases also the base stacking interactions. Concomitantly, vibrations at 860 and 1069 $cm^{-1}$, a characteristic of the A form of the dsDNA, progressively disappear, whereas those characteristic of the B form, such as the sugar-phosphate vibration at 836 and 1055 $cm^{-1}$, become fully stabilized. In the crossover range with comparable added Mg and intrinsic DNA ions ($[Mg]/[P] \approx 1$), the B form of dsDNA remains completely stable; spectra of the asymmetric $PO_2$ stretching mode (1234), the carbonyl C=O (1704) and the C=N (1608) in-plane stretching mode show a moderate intensity change as well as a prominent blue shift, indicating a stiffer interaction potential in the backbone and the nitrogen base regions due purely to a modified Debye screening when monovalent ions are substituted by divalent ones. Once non-physiological conditions at high added salt limit ($[Mg]/[P] > 10$) are established, vibrational spectra are strongly perturbed and show a striking intensity rise. These results consistently demonstrate that modest amounts of added magnesium ions interact with DNA prevalently via long-range but non-specific electrostatic interaction, first at the level of the phosphate groups and then also in the base region, and in this way stabilize the dsDNA in the B conformation. Conversely, in the presence of extremely high magnesium content that lead to overwhelming Debye screening, and with strongly perturbed hydration shell water, the secondary structure of dsDNA becomes severely modified. These results demonstrate that an interplay of the long-range electrostatic and short-range hydration forces may be of the primary importance in determination of the secondary structure of the dsDNA double helix. We argue that the observed effects at high [Mg] extreme conditions can be rationalized by invoking a structural phase transition of DNA into a compact form. Experiments such as atomic force microscopy, light scattering and circular dichroism combined with first principles density functional and molecular dynamics calculations are envisaged as desirable tools to elucidate our proposal.

## ACKNOWLEDGEMENTS

We thank M. Kosović for help in the data analysis, T. Ivek for help in editing the figures and V. Svetličić for very useful discussions. DFT calculations of the optimized structures and vibrations on a two A-T base pair fragment done by N. Došlić and M. Sapunar are greatly acknowledged.

## FUNDING

Funding for open access charge: School of Medicine, University of Zagreb.
*Conflict of interest statement.* None declared.

## REFERENCES

1. van der Maarel,J.R.C. (2008) *Introduction to Biopolymer Physics*. World Scientific.
2. Naji,A., Kanduc,M., Netz,R.R. and Podgornik,R. (2010) In: Hu,W-B and Shi,A-C (eds). *Understanding Soft Condensed Matter via Modeling and Computations*. World Scientific, Singapore, p. 265.
3. Dobrynin,A.V. and Rubinstein,M. (2005) Theory of polyelectrolytes in solutions and at surfaces. *Prog. Polym. Sci.*, **30**, 1049–1118.
4. Cherstvy,A.G. (2011) Electrostatic interactions in biological DNA-related systems. *Phys. Chem. Chem. Phys.*, **13**, 9942–9968.
5. Kanduc,M., Naji,A. and Podgornik,R. (2010) Counterion-mediated weak and strong coupling electrostatic interaction between like-charged cylindrical dielectrics. *J. Chem. Phys.*, **132**, 224703.
6. Netz,R.R. and Andelman,D. (2003) Neutral and charged polymers at interfaces. *Phys. Rep.*, **380**, 1–95.
7. Valle,F., Favre,M., De Los Rios,P., Rosa,A. and Dietler,G. (2005) Scaling exponents and probability distributions of DNA end-to-end distance. *Phys. Rev. Lett.*, **95**, 158105.
8. Boroudjerdi,H., Kim,Y.W., Naji,A., Netz,R.R., Schlagberger,X. and Serr,A. (2005) Statics and dynamics of strongly charged soft matter. *Phys. Rep.*, **416**, 129–199.
9. Hansen,P.L., Svensek,D., Parsegian,V.A. and Podgornik,R. (1999) Buckling, fluctuations, and collapse in semiflexible polyelectrolytes. *Phys. Rev. E*, **60**, 1956–1966.
10. Hud,N.V. and Vilfan,I.D. (2005) TOROIDAL DNA CONDENSATES: unraveling the fine structure and the role of nucleation in determining size. *Annu. Rev. Biophys. Biom.*, **34**, 295–318.
11. Bloomfield,V.A., Crothers,D.M. and Tinocco,I. (2000) *Nucleic Acids: Structures, Properties and Functions*. University Science Books, Sausalito.
12. Bloomfield,V.A. (1997) DNA condensation by multivalent cations. *Biopolymers*, **44**, 269–282.
13. Letellier,R., Ghomi,M. and Taillandier,E. (1987) Interpretation of DNA vibration modes II-the adenosine and thymidine residues involved in oligonucleotides and polynucleotides. *J. Biomol. Struct. Dyn.*, **4**, 663–683.
14. Letellier,R., Ghomi,M. and Taillandier,E. (1989) Interpretation of DNA vibration modes: IV - a single-helical approach to assign the phosphate-backbone contribution to the vibrational spectra in A and B conformations. *J. Biomol. Struct. Dyn.*, **6**, 755–768.
15. Letellier,R., Ghomi,M. and Taillandier,E. (1986) Interpretation of DNA Vibration Modes: I-The guanosine and cytidine residues involved in Poly(dG-dC).Poly(dG-dC) and d(CG)3.d(CG)3. *J. Biomol. Struct. Dyn*, **3**, 671–687.
16. Krummel,A.T. and Zanni,M.T. (2006) Interpreting DNA vibrational circular dichroism spectra using a coupling model from two-dimensional infrared spectroscopy. *J. Phys. Chem. B*, **110**, 24720–24727.
17. Tsuboi,M. (1970) Application of infrared spectroscopy to structure studies of nucleic acids. *Appl. Spectrosc. Rev.*, **3**, 45–90.
18. Every,A.E. and Russu,I.M. (2007) Probing the role of hydrogen bonds in the stability of base pairs in double-helical DNA. *Biopolymers*, **87**, 165–173.
19. Mak,C.H. (2016) Unraveling base stacking driving forces in DNA. *J. Phys. Chem. B*,**120**, 6010–6020.

20. Eichhorn,G.L. (1962) Metal Ions as stabilizers or destablizers of deoxyribonucleic acid structure. *Nature*, **194**, 474–475.
21. Clement,R.M., Sturm,J. and Daune,M.P. (1973) Interaction of metallic cations with DNA VI. Specific binding of Mg++ and Mn++. *Biopolymers*, **12**, 405–421.
22. Zimmer,C., Luck,G. and Triebel,H. (1974) Conformation and reactivity of DNA. IV. Base binding ability of transition-metal ions to native DNA and effect on helix conformation with special reference to DNA-Zn(II) complex. *Biopolymers*, **13**, 425–453.
23. Taboury,J.A., Bourtayre,P., Liquier,J. and Taillandier,E. (1984) Interaction of Z form poly(dG-dC).Poly(dG-dC) with divalent metal ions: localization of the binding sites by I.R. spectroscopy. *Nucleic Acids Res.*, **12**, 4247–4258.
24. Duguid,J., Bloomfield,V.A., Benevides,J. and Thomas,G.J. (1993) Raman spectroscopy of DNA-metal complexes. I. Interactions and conformational effects of the divalent cations: Mg, Ca, Sr, Ba, Mn, Co, Ni, Cu, Pd, and Cd. *Biophys. J.*, **65**, 1916–1928.
25. Bhattacharyya,R.G., Nayak,K.K. and Chakrabarty,A.N. (1988) Interaction of MgATP2- with DNA: assessment of metal-binding sites and DNA conformations by spectroscopic and thermal denaturation studies. *Inorg. Chim. Acta*, **153**, 79–86.
26. Ahmad,R., Arakawa,H. and Tajmir-Riahi,H.A. (2003) A comparative study of DNA complexation with Mg(II) and Ca(II) in aqueous solution: major and minor grooves bindings. *Biophys. J.*, **84**, 2460–2466.
27. Langlais,M., Tajmir-Riahi,H.A. and Savoie,R. (1990) Raman spectroscopic study of the effects of Ca2+, Mg2+, Zn2+, and Cd2+ ions on calf thymus DNA: binding sites and conformational changes. *Biopolymers*, **30**, 743–752.
28. Misra,V.K. and Draper,D.E. (1999) The interpretation of Mg2+ binding isotherms for nucleic acids using Poisson-Boltzmann theory. *J. Mol. Biol.*, **294**, 1135–1147.
29. Yoo,J. and Aksimentiev,A. (2012) Competitive binding of cations to duplex DNA revealed through molecular dynamics simulations. *J. Phys. Chem. B*, **116**, 12946–12954.
30. Tomic,S., Grgicin,D., Ivek,T., Vuletic,T., Babic,S.D. and Podgornik,R. (2012) Dynamics and structure of biopolyelectrolytes in repulsion regime characterized by dielectric spectroscopy. *Physica B*, **407**, 1958–1963.
31. Bai,Y., Greenfeld,M., Travers,K.J., Chu,V.B., Lipfert,J., Doniach,S. and Herschlag,D. (2007) Quantitative and comprehensive decomposition of the ion atmosphere around nucleic acids. *J. Am. Chem. Soc.*, **129**, 14981–14988.
32. Tomic,S., Babic,S.D., Vuletic,T., Krca,S., Ivankovic,D., Griparic,L. and Podgornik,R. (2007) Dielectric relaxation of DNA aqueous solutions. *Phys. Rev. E*, **75**, 021905.
33. Record,M.T. (1975) Effects of Na+ and Mg++ ions on helix-coil transition of DNA. *Biopolymers*, **14**, 2137–2158.
34. Dolanski Babić,S. (2008) doctoral thesis, University of Zagreb.
35. Pohle,W., Bohl,M. and Bohlig,H. (1990) Interpretation of the influence of hydrogen bonding on the stretching vibrations of the $PO_2^-$ moiety. *J. Mol. Struct.*, **242**, 333–342.
36. Arakawa,H., Ahmad,R., Naoui,M. and Tajmir-Riahi,H.A. (2000) A comparative study of calf thymus DNA binding to Cr(III) and Cr(VI) ions - Evidence for the guanine N-7-chromium-phosphate chelate formation. *J. Biol. Chem.*, **275**, 10150–10153.
37. Ouameur,A.A. and Tajmir-Riahi,H.A. (2004) Structural analysis of DNA interactions with biogenic polyamines and cobalt(III)hexamine studied by Fourier transform infrared and capillary electrophoresis. *J. Biol. Chem.*, **279**, 42041–42054.
38. Champeil,P., Tran,T.P.L. and Brahms,J. (1973) New approach to characterization of B-forms and A-forms of DNA by IR spectroscopy. *Biochem. Biophys. Res. Commun.*, **55**, 881–887.
39. Dirico,D.E., Keller,P.B. and Hartman,K.A. (1985) The infrared-spectrum and structure of the type-I complex of silver and DNA. *Nucleic Acids Res.*, **13**, 251–260.
40. Keller,P.B. and Hartman,K.A. (1986) The effect of ionic environment and mercury(II) binding on the alternative structures of DNA. An infrared spectroscopic study. *Spectrochim. Acta A*, **42**, 299–306.
41. Neault,J.F. and Tajmir-Riahi,H.A. (1999) Structural analysis of DNA-chlorophyll complexes by Fourier transform infrared difference spectroscopy. *Biophys. J*, **76**, 2177–2182.
42. Banyay,M., Sarkar,M. and Graslund,A. (2003) A library of IR bands of nucleic acids in solution. *Biophys. Chem.*, **104**, 477–488.
43. Gomes,P.J., Ribeiro,P.A., Shaw,D., Mason,N.J. and Raposo,M. (2009) UV degradation of deoxyribonucleic acid. *Polym. Degrad. Stabil.*, **94**, 2134–2141.
44. Taillandier,E., Fort,L., Liquier,J., Couppez,M. and Sautiere,P. (1984) Role of the protein-alpha helixes in histone DNA interactions studied by vibrational spectroscopy. *Biochemistry-US*, **23**, 2644–2650.
45. Liquiers,J., Taillandier,E., Peticolas,W.L. and Thomas,G.A. (1990) The infrared and Raman spectra of the duplex of d(GGTATACC) in the crystal show bands due to both the A-form and the B-form of DNA. *J. Biomol. Struct. Dyn.*, **8**, 295–302.
46. Matsui,H., Toyota,N., Nagatori,M., Sakamoto,H. and Mizoguchi,K. (2009) Infrared spectroscopic studies on incorporating the effect of metallic ions into a M-DNA double helix. *Phys. Rev. B*, **79**, 235201.
47. Manning,G.S. (1978) Molecular theory of polyelectrolyte solutions with applications to electrostatic properties of polynucleotides. *Q. Rev. Biophys.*, **11**, 179–246.
48. Lipfert,J., Doniach,S., Das,R. and Herschlag,D. (2014) Understanding nucleic acid-ion interactions. *Annu. Rev. Biochem.*, **83**, 813–841.
49. Skerjanc,J. and Strauss,U.P. (1968) Interactions of polyelectrolytes with simple electrolytes. III. The binding of magnesium ion by deoxyribonucleic acid. *J. Am. Chem. Soc.*, **90**, 3081–3085.
50. Tajmir-Riahi,H.A., Naoui,M. and Ahmad,R. (1993) The effects of Cu2+ and Pb2+ on the solution structure of calf thymus DNA-DNA condensation and denaturation studied by Fourier-transform IR difference spectroscopy. *Biopolymers*, **33**, 1819–1827.
51. Tajmir-Riahi,H.A., Ahmad,R. and Naoui,M. (1993) Interaction of calf-thymus DNA with trivalent La, Eu, and Tb ions-metal-ion binding, DNA condensation and structural features. *J. Biomol. Struct. Dyn.*, **10**, 865–877.
52. Omerzu,A., Mihailovic,D., Anzelak,B. and Turel,I. (2007) Optical spectra of wet and dry M-DNA. *Phys. Rev. B*, **75**, 121103.
53. Hackl,E.V., Kornilova,S.V., Kapinos,L.E., Andrushchenko,V.V., Galkin,V.L., Grigoriev,D.N. and Blagoi,Y.P. (1997) Study of Ca2+, Mn2+ and Cu2+ binding to DNA in solution by means of IR spectroscopy. *J. Mol. Struct.*, **408**, 229–232.
54. Koltover,I., Wagner,K. and Safinya,C.R. (2000) DNA condensation in two dimensions. *Proc. Natl. Acad. Sci. U.S.A.*, **97**, 14046–14051.
55. Sun,X.G., Cao,E.H., Zhang,X.Y., Liu,D.G. and Bai,C.L. (2002) The divalent cation-induced DNA condensation studied by atomic force microscopy and spectra analysis. *Inorg. Chem. Commun.*, **5**, 181–186.
56. Shaw,S.Y. and Wang,J.C. (1993) Knotting of a DNA Chain during Ring-Closure. *Science*, **260**, 533–536.
57. Rau,D.C. and Parsegian,V.A. (1992) Direct measurement of the intermolecular forces between counterion-condensed DNA double helices - evidence for long-range attractive hydration forces. *Biophys. J.*, **61**, 246–259.
58. Timsit,Y., Westhof,E., Fuchs,R.P.P. and Moras,D. (1989) Unusual helical packing in crystals of DNA bearing a mutation hot spot. *Nature*, **341**, 459–462.
59. Naji,A., Kanduc,M., Forsman,J. and Podgornik,R. (2013) Perspective: Coulomb fluids-Weak coupling, strong coupling, in between and beyond. *J. Chem. Phys.*, **139**, 150901.
60. Ben-Yaakov,D., Andelman,D., Podgornik,R. and Harries,D. (2011) Ion-specific hydration effects: extending the Poisson-Boltzmann theory. *Curr. Opin. Colloid. In.*, **16**, 542–550.
61. Manning,G.S. (1977) Limiting laws and counterion condensation in polyelectrolyte solutions .4. Approach to limit and extraordinary stability of charge fraction. *Biophys. Chem.*, **7**, 95–102.
62. Wilson,R.W. and Bloomfield,V.A. (1979) Counter-ion-induced condensation of deoxyribonucleic-acid - light-scattering study. *Biochemistry-US*, **18**, 2192–2196.
63. Polyanichko,A.M., Andrushchenko,V.V., Chikhirzhina,E.V., Vorob'ev,V.I. and Wieser,H. (2004) The effect of manganese(II) on DNA structure: electronic and vibrational circular dichroism studies. *Nucleic Acids Res.*, **32**, 989–996.